Solid State Electrolyte to Enable Structural **Supercapacitors**

Nandu Koripally¹, Lulu Yao², Jason D. Azoulay³, Tse Nga Ng^{1,2} ¹Department of Electrical and Computer Engineering, University of California San Diego, La Jolla, CA, USA ²Materials Science Engineering Program, University of California San Diego, La Jolla, CA, USA ³Chemisty Department, Georgia Institute of Technology, Atlanta, GA, USA e-mail: tnn046@ucsd.edu

Abstract—Supercapacitors are known for longer cycle life and faster charging rate compared to batteries. However, the energy density of supercapacitors requires improvement to expand their application space. To raise the energy density of structural supercapacitors, this work demonstrates a low resistance and mechanically strong solid-state electrolyte.

Keywords—supercapacitors, solid-state electrolyte, energy storage

I. Introduction

Supercapacitors are electrochemical energy storage systems that outperform batteries in power density and cycle lifetime [1-5]. However, their lower energy density is a limiting factor in implementation. One way to realize a high energy density is to use structural supercapacitors [6]. Fig. 1A shows the composition of a structural supercapacitor. They typically integrate load-bearing carbon fiber electrodes with active redox material and a solid-state electrolyte into a multifunctional structure. Since the materials are integrated into the structure, they have room to hold more active material while reducing unnecessary device weight to increase the energy density and take advantage of supercapacitors' power density and cycle lifetime. This design is applicable to the transportation sector where boats and cars already incorporate carbon composites. Fig. 1A shows the realization of a boat hull made of supercapacitor materials [6].

The most important part of the structural supercapacitor is the electrode-electrolyte interface. Here, the solid-state electrolyte (SSE) must be ionically conductive to allow charge exchange yet strong enough to support the electrodes and any additional weight that may be placed on the device. These have an inverse relationship and other groups have favored mechanical strength leading to low electrochemical performance [7-11].

The ionic conductivity is determined by using Eq. (1) where L = device thickness, R = equivalent series resistance (ESR) and A = device area. If the device thickness and area are fixed, the conductivity is dependent on decreasing the equivalent series resistance of the device. This measurement is done by taking the electrochemical impedance spectroscopy (EIS) to analyze the electrode-separator surface.

$$\sigma = \frac{L*R}{4} \tag{1}$$

In this work, we design and optimize a SSE to improve its ionic conductivity while maintaining the mechanical strength. Then we incorporated it into a structural supercapacitor as a proof-of-concept demonstration.

DEVICE FABRICATION AND CHARACTERIZATION

A. Materials for Solid-State Electrolyte

Typical materials for solid-state electrolytes in Li-ion batteries are sulfides, oxides, and solid polymer based electrolytes [12,13]. Sulfide and oxide based solid state electrolytes have a high ionic conductivity, but they have poor contact at the interface and their fabrication is more complex.

Solid polymer electrolytes are easier to fabricate and have, but their conductivity is 3-5 magnitudes lower than liquid electrolytes [12]. Among these, epoxy mixtures with PVDF-HFP and PEO (Fig. 1B) are widely used for their high electrolyte salt uptake [11,12]. We chose these polymers and tested their ionic conductivity and mechanical properties. Fig. 1. (a) Structural supercapacitor diagram and structural boat hull [6]. (b)

Carbon fiber electrode Separator/ PVDF-HFP/ ероху electrolyte @ ²⁰ PEO PVDF-HE 0 Z'(Ω)

Chemical structures of PVDF-HFP and PEO. (c) Structural electrolyte matrix. (d) Chemical structure of redox polymer QxTh [5,6]. (e) Electrochemical impedance spectroscopy (EIS) of PVDF-HFP and PEO solid state electrolytes

B. Preparing Solid-State Electrolyte

The electrolyte fabrication was conducted inside a nitrogen filled glovebox. A solution of poly(vinylidene fluoride-cohexafluoropropylene) (PVDF-HFP) and solvent N-methyl-2pyrrolidone (NMP) was prepared in a 1:4 weight ratio. A solution of polyethylene oxide (PEO) and solvent acetonitrile (ACN) was prepared in a 1:10 weight ratio. These polymer solutions were then separately mixed with commercial epoxy and electrolyte tetraethylammonium tetrafluoroborate liquid electrolyte 0.5M (TEABF₄) with PC in a 1:4:1 weight ratio. The commercial epoxy forms a structural matrix and the TEABF₄ transported through the PVDF-HFP or PEO pathways boosts ionic conductivity.

C. Device Fabrication

The structural electrodes were made using carbon fiber and the separator was cellulose paper. The cellulose paper served as the structure onto which the uncured epoxy was deposited to form the SSE. The carbon fiber electrodes are mechanically strong and conductive to support the full device. These carbon fiber electrodes were coated in the polymer 4,6,7,9-tetra(thiophen-2-yl)-[1,2,5]thiadiazolo[3,4-g]quinoxaline (QxTh) and annealed at 200°C for 30 minutes inside the glovebox. The redox polymer QxTh shown in Fig. 1D [5,6] has a wide 3V potential window that would boost the device capacitance.

After preparing the electrodes, the epoxy SSE was placed between the carbon fiber electrodes to form a bonded laminate. Then the device was annealed at 70°C for 30 minutes.

Fig. 1E shows the EIS results of the structural supercapacitor without active material on the electrodes to analyze only the electrolyte. The electrolyte with PEO additive has an ESR of 7.79 Ω and the SSE with PVDF-HFP additive has an ESR of 19.85 Ω .

D. Strength Tests

The same devices were used for flexural and tensile stress tests following the EIS measurements. The flexural strength test (Fig. 2A) held the sample and added force to the center until the sample broke. The tensile strength test (Fig. 2C) held the sample and pulled it until device layers delaminated and fell apart. For the tests we established a baseline with carbon fiber electrodes, the cellulose separator, and only commercial epoxy. Then we tested the structures using SSEs with the additives of PVDF-HFP or PEO.

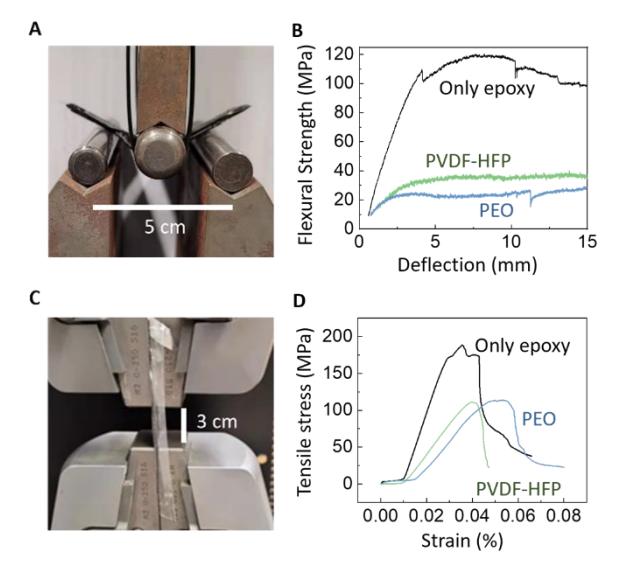


Fig. 2. (a) Structural supercapacitor in a flexural strength test. (b) Flexural strength curves for structural supercapacitors bonded by SSEs. (c) Structural

supercapacitor in a tensile strength test. (d) Tensile strength curves of structural supercapacitors bonded by different SSEs.

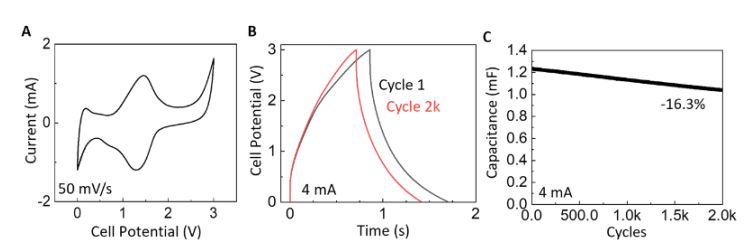
Fig. 2B shows the maximum flexural strength of the structures with baseline epoxy alone, with PVDF-HFP, and with PEO at 119 MPa, 35 MPa, and 24 MPa, respectively. **Fig. 2C** shows the maximum tensile strength at 188 MPa for the baseline epoxy, 111 MPa for the sample with PVDF-HFP, and 113 MPa for the sample with PEO.

III. DATA ANALYSIS AND DISCUSSION

The structural supercapacitors using SSE added with PEO had half the ESR of the one with PVDF-HFP. The PEO additive provided more channels for ion diffusion from the electrolyte. Since our goal is to increase ionic conductivity, we chose to use PEO as our additive. The tensile strength of both additives was expected to be lower than pure epoxy due to the diluted epoxy ratio, they both had a similar tensile strength. Meanwhile, the flexural strength was only slightly higher with PVDF-HPE compared to PEO. Additionally, the NMP solvent for PVDF-HPE was corrosive to the QxTh polymer on the carbon fibers. The ACN solvent for PEO is compatible with QxTh.

Finally, we examined the electrochemical properties of the structural supercapacitor using carbon fiber electrodes with a 2 mg/cm² loading of QxTh and the SSE with PEO. Fig. 2A shows the cyclic voltammetry (CV) curve of the device over a 3V window. The device maintains its redox kinetics which are shown through the symmetric peaks. Fig. 2B and Fig. 2C show the galvanostatic charge-discharge (GCD) curve and the calculated device capacitance over 2,000 cycles. The device retains 83% of its capacity, showing stable performance on par with monofunctional supercapacitors.

Fig. 3. (a) Cyclic voltammetry (CV) of structural supercapacitor with PEO SSE.



(b) Galvanostatic charge-discharge (GCD) curves of structural supercapacitor with PEO SSE. (c) Capacitance retention of structural cell with PEO-cellulose separator.

The energy stored in a supercapacitor is determined by using Eq. (2) [14] in galvanostatic charge-discharge measurements:

$$E = \frac{1}{A} \int_0^{t_d} V dt \tag{2}$$

where A = device area, t_d = discharge time, and V = potential. The calculated energy density using the GCD curves from **Fig. 3B** and **Eq. (2)** is 0.59 uWh/cm² at 2,000 cycles. The power density, calculated by **Eq. (3)** [14] is 3 mW/cm².

$$P = \frac{E}{t_d} \tag{3}$$

IV. CONCLUSION

This work demonstrated a solid-state electrolyte with a low contact interface contact resistance of 7.79Ω , maximum flexural strength of 24 MPa, and a maximum tensile strength of 113 MPa. This PEO-epoxy matrix design allowed incorporation into a structural supercapacitor with reversible redox reactions, achieving a baseline power density of 3 mW/cm², energy density of 0.59 uWh/cm², and a cycling stability of 2,000 cycles.

The successful implementation of this electrolyte and structural design opens new avenues in further improving the performance of energy storage supercapacitors.

ACKNOWLEDGMENT

The authors are grateful for the support from National Science Foundation PFI-2120103 and MCA-2120701. Parts of the work was performed at the San Diego Nanotechnology Infrastructure of UCSD, which is supported by NSF EECS-1542-148.

REFERENCES

- Fleischmann, S., Mitchell, J.B., Wang, R., Zhan, C., Jiang, D., Presser, V., and Augustyn, V. (2020). Pseudocapacitance: from fundamental understanding to high power energy storage materials. Chem. Rev. 120, 6738–6782.
- [2] Simon, P., and Gogotsi, Y. (2020). Perspectives for electrochemical capacitors and related devices. Nat. Mater. 19, 1151–1163.
- [3] Shin, C., Yao, L., Jeong, S.-Y., and Ng, T.N. (2024). Zinc-copper dualion electrolytes to suppress dendritic growth and increase anode utilization in zinc ion capacitors. Sci. Adv.10, eadf9951.
- [4] Shin, C., Yao, L., Lin, H., Liu, P., and Ng, T.N. (2023). Photothermal supercapacitors with gel polymer electrolytes for wide temperature range operation. ACS Energy Lett. 8, 4, 1911–1918.
- [5] Yao, L., Liu, J., Eedugurala, N., Mahalingavelar, P., Adams, D. J., Wang, K., Mayer, K. S., Azoulay, J. D., and Ng, T. N. Ultrafast High-Energy Micro-Supercapacitors Based on OpenShell Polymer-Graphene Composites. Cell Reports Physical Science 2022, 100792.
- [6] Yao, L., Zheng, K., Koripally, N., Eedugurala, N., Azoulay, J. D., Zhang, X., and Ng, T. N. (2023). Structural pseudocapacitors with reinforced interfaces to increase multifunctional efficiency. Sci. Adv. 9, eadh0069.
- [7] Asp, L.E., et al. (2021). A structural battery and its multifunctional performance. Adv. Energy Sustain. Res 2, 2000093.
- [8] Javaid, A., Ho, K. K. C., Bismarck, A., Steinke, J. H. G., Shaffer, M. S. P., and Greenhalgh, E. S. (2018). Improving the multifunctional

- behaviour of structural supercapacitors by incorporating chemically activated carbon fibres and mesoporous silica particles as reinforcement. Compos. Mater. 52, 3085–3097.
- [9] Chopade, S. A., Au, J. G., Li, Z., Schmidt, P. W., Hillmyer, M. A., and Lodge, T. P. (2018). Robust polymer electrolyte membranes with high ambient-temperature lithium-ion conductivity via polymerizationinduced microphase separation. ACS Appl. Mater. Interfaces 10, 35108– 35117.
- [10] Fan, L.-Z., He, H., and Nan, C.-W. (2021). Tailoring inorganic-polymer composites for the mass production of solid-state batteries. Nature Reviews Materials. 6, 1003–1019.
- [11] Zheng, Y., et al. (2020). A review of composite solid-state electrolytes for lithium batteries: fundamentals, key materials and advanced structures. Chem. Soc. Rev. 49, 8790–8839.
- [12] Zhao, Q., Stalin, S., Zhao, C.-Z., and Archer, L. A. (2020). Designing solid-state electrolytes for safe, energy-dense batteries. Nature Reviews Materials 5.3 229-252.
- [13] Chen, L., Huang, Y.-F., Ma, J., Ling, H., Kang, F., and He, Y.-B. (2020). Progress and perspective of all-solid-state lithium batteries with high performance at room temperature. Energy Fuels 2020, 34, 11, 13456– 13472
- [14] Li, X., Li, H., Fan, X., Shi, X., and Liang, J. (2020). 3D-Printed stretchable micro-supercapacitor with remarkable areal performance. Adv. Energy Mater. 10, 1903794.